

Plastic Instability Test of Elbows Under In-Plane and Out-of-Plane Bending

A. Imazu, Y. Sakakibara, T. Nagata

*Power Reactor and Nuclear Fuel Development Corporation,
Oarai Engineering Center, Oarai, Ibaraki-ken 311-13, Japan*

T. Hashimoto

*Engineering Dept., Tokyo Design Office,
Kawasaki Heavy Industries, Ltd., 2-4-25 Minami-suna,
Koto-ku, Tokyo, Japan*

In the thin-walled elbows of LMFBR piping operating at elevated temperatures, cares must be taken to buckling or instability due to short term as well as long term loadings.

Plastic instability tests or plastic buckling tests were conducted on 12 inches Sch. 10S and Sch. 20S long elbow models (total 5 models) made of type 304 stainless steel. The test temperature was 600°C and the loading modes adopted were in-plane and out-of-plane moment loadings. Measured were temperature, load, displacement at the loaded end, rotation of elbows, rotation per unit bend angle of elbows, ovality of cross-section of elbows and strain. The tests were performed far beyond the plastic instability point by controlling the displacement at the loaded end of the models.

The plastic instability occurred when elbows rotated by approximately 6 degrees irrespective of loading mode and dimensions of elbows. Torsional moment was inevitably incorporated in the test under out-of-plane bending. The plastic instability took place at nearly the same moment level under both in-plane and out-of plane bendings. This means that torsional moment has a negligible effect on the plastic buckling.

Nearly linear relationship was observed between the displacement of the loaded end and any other measured value such as the rotation throughout the entire elbows (bend angle of 90 degrees), the rotation per unit bend angle at the center part of 90 degrees elbows, and the radial displacements of the elbow cross-sections, even under the load condition where plastic deformation was significant. Such tendency was found in the inelastic analysis reported in a reference.

A variety of methods have been proposed for the determination of collapse loads. They were applied to the experimental results. The method given in ASME Section III Appendix F will be the most suitable one in these particular cases. ASME Section III provides the simplified design rule for piping. The criteria for the primary stresses were examined by comparing with actually observed behaviors. It can be said that adequate design margin is not incorporated in the provision for Level D service limit included in Appendix F, if the rule is applied at 600°C. The plastic large deformation behavior was compared to creep deformation. It was concluded that they were similar in a global sense.

T. Nagata :

Presently with FBR Development Project, Headquarters, Power Reactor and Nuclear Fuel Development Corporation, 1-9-13 Akasaka, Minatoku, Tokyo, Japan

1. Introduction

Pipe elbows are widely used in piping systems to accommodate thermal expansion, because they are, in usual cases, the most flexible members in piping systems. However cares must be taken to avoid instability due to short term as well as long term loadings.

A series of creep tests of elbows including creep buckling tests have been conducted [1] [2] [3] and a simplified method of creep buckling analysis of elbows under in-plane bending has been developed in Japan[2]. As for plastic instability or buckling, on the other hand, little data are available. The extensive experimental works were performed on carbon steel and stainless steel elbows by Greenstreet [4]. All tests were conducted at room temperature and most of them were terminated below instability load. Sobel and Newman reported the detailed plastic large deformation analysis of an elbow [5].

This paper describes the plastic instability tests on LMFBR piping elbows at 600°C. Four elbows were tested under in-plane moment and one under out-of plane moment. Plastic large deformation and instability behaviors of elbows were investigated and compared with creep deformation and buckling. Test results were examined in terms of limits on primary stresses.

2. Test set-up and testing procedure

Fig. 1 illustrates the set-up for testing which consists of an electro-hydraulic servo-controlled actuator, an loading frame, fixtures, electric heaters and data acquisition unit.

The actuator is connected to one end of a specimen, with the other end fixed to the frame rigidly through a fixture. Shear force is applied to a specimen by the actuator. Fig. 1 shows the arrangement for in-plane moment loading and load is imposed in such a direction that closes the elbow. The actuator is placed in the direction perpendicular to the paper under out-of-plane moment loading. Therefore torsional moment is inevitably incorporated in this case. The actuator has the maximum stroke of 500mm, which is sufficient for the plastic instability tests. The displacement at the loaded end of a specimen is increased at a constant rate and reaches the maximum value (500mm) in half an hour. The electric heaters are divided into twelve blocks and inserted inside the specimen. Each block is controlled independently to achieve uniform temperature distribution over the elbow part. An example of specimens is shown in Fig. 2. A 12-inches Sch. 20 or Sch. 10 type 304 stainless steel long elbow is welded to straight pipes. The notations for θ and ϕ are also given in Fig. 2.

Different set-up was also used for one test (BE-306). It is composed of heating system which heats a specimen by circulating hot air inside the specimen, and loading system by dead weight. Effect of dead weight of the specimen, heaters, thermal insulator and other devices for instrumentation was cancelled by applying counterbalance weight in some tests in which the effect is expected to be rather large. In other tests, the effect was excluded in a calculational way. All data are continuously recorded on a magnetic tape or paper tape. The symbol of specimens and the test conditions are summarized in Table 1. Those for related creep buckling tests are also depicted in Table 1.

3. Instrumentation

Applied load was measured by a load cell. The displacement at the loaded end (δ_0) was measured by a displacement transducer. Rotation of an elbow (γ_e) was measured by several sets of displacement transducers attached at both ends of the elbow. In some tests, rotation of an elbow was calculated from the displacement at the loaded end. Rotations per unit bend

angle of an elbow were (ω) obtained from two sets of displacements ($\delta\omega$) as can be seen in Fig.1. Ovalization of the elbow at $\phi = 0^\circ$ cross-section was measured a specially designed device. It consists of a rigid ring frame, springs, sensoring rods and displacement transducers. The sensoring rods are placed at 15° or 30° interval around the circumference. Their movements are measured by displacement transducers. Strains are measured on inside and outside surfaces of $\theta = 95^\circ$ and 265° at $\phi = 0^\circ$ crosssection of the elbow, where the maximum strains occur. Resistance type high temperature strain gages, ALLTECH SG-425 were adopted for the test.

4. Test results

Linear relationship was observed between the displacement at the loaded end (δ_0) and the rotation throughout the entire elbow (γ_e). It also held between δ_0 and rather local displacements $\delta\omega$ or the rotation of elbow per unit bend angle (ω). This implies that significant elastic follow-up is observed neither in the elbow-straight pipes assembly nor in the elbow itself. Bending moment varies over the axis of bend both for in-plane and out-of plane bending. The equivalent or average moment was used for the former and moment at the center of the elbow was adopted for the latter case as a representative value of moment. Fig. 3 and Fig. 4 are the relation between γ_e and moment for in-plane bending and out of plane bending, respectively. In the latter case, resultant moment and its out-ofplane component are shown as moment. First the elbow shows purely elastic response and it is followed by predominantly plastic deformation. The nonlinear response becomes increasingly larger. The moment reaches the maximum value at six or seven degrees of rotation of elbow for both in-plane and out-of plane bendings, and this load is defined as the plastic instability load or plastic buckling load. After then moment decreases gradually. Out-of plane moment component at the plastic instability point is nearly the same as in-plane moment. This means torsional moment component has a negligible effect on plastic instability.

Fig. 5 is the distribution of radial displacements along the circumference for various levels of deformation under in-plane bending (BE-308B). The maximum value appears at $\theta = 95^\circ$ or 265° . It corresponds to the location where the maximum strain occurs. Fig. 6 shows the same relation as Fig. 5 in normalized value by radial displacement at $\theta = 95^\circ$. The data of creep buckling test on Sch. 20 elbow (BE-304) are also plotted in the figure. It is of interest to note that deformation pattern of elbow is nearly the same for every degree of plastic deformation and types of deformation (plastic and creep). On the other hand, some degrees of concentration of deformation was observed around $\theta = 95^\circ$ with increase of δ_0 in the calculation by FEM computer code 'FINAS'[6].

The radial displacements at the crown ($\theta = 90^\circ$) are depicted against the rotations of elbows for plastic deformation of the thick elbow (BE-305) and the thin elbow (BE-308B) in Fig. 7. The results of creep buckling test on the thick elbow (BE-307) and numerical calculation in a reference [5] are also shown in the same figure for comparison. Nearly linear relation is observed between the radial displacements and the rotations of elbows for all cases. More exactly, the slopes decrease in the region where inelastic deformation is dominant. In other words, the change of cross-sectional deformation for prescribed increment of rotation of elbow is smaller in inelastic response than in elastic response. This fact is deduced by referring to Fig. 6 as well. Such tendency is more significant in case of thin elbows. Results on plastic (BE-305) and creep (BE-307) tests on specimens with nearly the same dimensions exhibit very similar behaviors, though some experimental errors are expected

at the stage of small displacement. Inelastic analysis for plastic deformation by 'MARC' which takes into consideration large displacement effect displays similar behaviors. Theoretical analysis by 'FINAS' was also conducted for the same problem as 'MARC'. The solution based on small displacement theory showed the linear relation between rotation and radial displacement, while calculation which includes the effect of large displacement exhibited close response to MARC. Fig. 8 illustrates the change of ovality with rotation for plastic and creep tests on thick elbows and plastic test on a thin elbow. No remarkable difference is observed between plastic and creep deformations, as can be expected from Fig. 7. The curve of thin elbow is quite different from that of thick elbow. These facts correspond to the curves of BE-308B, BE-305 and BE-307 in Fig. 7. The cross-sections of elbows were calculated for different levels of deformations. Fig. 9 is an example for BE-308B. The assumption of inextensibility of the center line of cross-section was used in the calculation.

Fig. 10 shows the measured and calculated strains. Calculated strains were obtained from measured radial displacements based on small displacement thin shell theory and also by using the assumption of inextensibility at the center of cross-section. It is natural that the tendency of calculated strains is close to Fig. 7, because the pattern of distribution of radial displacements is unchanged by the displacement of the loaded end. Actually, geometric nonlinear effects are significant, therefore other terms should be introduced into the calculation. The calculated strains by 'FINAS' including large deformation effects exhibited significant strain concentration at larger values of δ_0 . Measured strains were obtained from the output of ALLTECH gages, the maximum specified measuring range of which is 0.6%. Therefore, the value over 0.6% is supposed to be almost unreliable. It became clear from similar tests that strains on outside surface are thirty to forty percents lower than those on inside surface. The discrepancy between measured and calculated strains in Fig. 10 can be said large, even if it is recognized that the calculated strains should correspond to the average values of strains on inside and outside surfaces.

5. Discussions

It was made clear that no significant difference is observed between plastic and creep deformations from the point of view of ovality. The condition for plastic or creep buckling of elbows would be mainly governed by this ovality and resulting stress distribution around the circumference and through the wall thickness. It is anticipated that there will be no remarkable difference in stress distributions between plastic and creep deformations. Fig. 11 illustrates the results of plastic instability test (BE-305) and creep buckling test (BE-307) of the similar elbows at 600°C. Initial response at the loading stage of BE-307 shows stiffer behavior than that of BE-305. The imaginary plastic response of BE-307 above point A is depicted by a dotted line. It is not so unnatural to assume that this line will go through the point B. Based on this fact and the above-mentioned discussion that the stress distribution will be similar between plastic and creep deformations, it might be expected that creep buckling will occur at $\delta_0 = \delta_{01}$ under load P_1 and at $\delta_0 = \delta_{02}$ under load P_2 , if creep buckling tests are conducted on BE-305 specimen.

ASME Sec. III [7] defines collapse load as "the load at which the deformations of an ideally plastic structure increase without bound", and it further mentions that collapse load should be calculated by the lower bound theorem of limit analysis. Collapse load is interpreted as a conceptual conservative substitute for the maximum carrying capacity of

structures, calculated by using simple procedure (ideally plastic material model and limit analysis) and conservative theory (lower bound theory). The logical conservatism inherent in collapse load might be violated if geometric nonlinear effects are significant; because limit analysis does not take these into account. In this case, collapse load determined by limit analysis might lose its positive meanings. Yield stress level to be used for calculation of collapse load especially for Level D Service Limits (P_c) is another important factor for the adequacy of the result of limit analysis.

A variety of methods have been proposed for defining plastic collapse load of components based on experimental data or inelastic analyses [8]. Fig. 12 illustrates schematically some methods for defining plastic collapse load. The authors are not aware of the background of these methods. P_c^A is collapse load adopted by ASME Section III. The methods shown in Fig. 12 and the so-called tangent method were applied to the experimental data. The tangent method was difficult to apply, because the tangent in the plastic region is not determined definitely as can be seen from Fig. 3 and Fig. 4. The collapse loads determined by various methods are depicted in Table 2 together with plastic instability loads. Table 2 contains the preliminary test results on a carbon steel elbow (BE-301). There would be no definite criteria for determining what is the most adequate method because of two problems, geometric non-linear effects and effective yield stress involved in limit analysis in these test cases. P_c^{β} has the lowest value. Roughly speaking, this load will cause the initial yielding in the structure. The collapse load should be higher than this load. P_c^A and P_c^{β} depend on the scale of the ordinate and abscissa. This is a logical problem associated with these two methods. Furthermore, P_c^{β} was determined by the intersection of the experimental curve with the straight line far beyond the plastic instability point. P_c^A adopted by ASME Sec. III seems to have no definite drawback and specifies the collapse load at the transition region. Incidentally, P_c^A nearly coincided with the lower bound collapse load after Spence and Findlay [9]. The design limits of primary load or stress for level D service limits are provided in ASME Sec. III Appendix F, where it could be judged that $0.9 P_c$ (collapse load) is equivalent to $0.7 P_I$ (plastic instability load). Hence P_c should be $0.7/0.9 \approx 0.78 P_I$. The values of P_c / P_I are around 0.7 except 0.95 for a carbon steel elbow in Table 2. From these facts, the method provided by ASME Sec. III seems to be the most suitable one for these specific test results on stainless steel elbows. Sec. III Appendix F describes the special rule for limits of primary load of piping for level D service condition, which is expressed by $B_2 \frac{D_0}{2I} M \leq 3 S_m$ for the special condition only moment loadings are applied. The column ⑥ in Table 2 shows the allowable load determined by the above equation based on S_m value specified in ASME Code Case N-47 [10]. No data satisfy the equation except data on a carbon steel elbow. One clear reason is that S_m (design stress intensity) is as high as $0.9 S_y$ (minimum yield strength) for austenitic stainless steel at higher temperatures. Another possible reason is that stress-strain curve of austenitic stainless steel is different from that of carbon steel in the region effective to collapse or in other words the effective yield stress might be lower than stress for 0.2% offset strain as pointed out by Greenstreet [4], especially at high temperatures. This fact will presumably intensify geometric nonlinear effects in such thin elbows as tested. The column ⑦ corresponds to the initial yield load calculated by a simple method of $C_2 \frac{D_0}{2I} M = 1.25 S_y$ given by ASME Sec. III NB 3600, where $1.25 S_y$ is expected to be average yield strength. The column ⑧ (P_c^A / P_y) is considered to be the shape factor of elbow. The ratio of collapse load of elbow to that of

straight pipe is depicted in column ⑩. The lack of conservatism for Level C and D Service Limits is discussed by Rodabaugh [11] for room temperature test data of stainless steel elbows of Greenstreet.

6. Conclusion

Plastic instability tests were conducted on five thin-walled type 304 stainless steel elbows at 600°C. Plastic instability occurred when elbows rotated by six to seven degrees under both in-plane and out-of-plane bendings. Nearly linear relation was observed between gross deformation parameter and more local parameters. Plastic large deformation behaviors were similar to creep deformation in a global sense. Collapse load defined in ASME Sec. III seems to be the most adequate one. The experimental results did not satisfy the rule for limits on primary stresses of pipings for level D service condition of ASME Sec. III, when this rule was applied to higher temperature. This will be attributed to the adopted S_m value as high as 0.9 S_y and presumably stress-strain curve of stainless steel at higher temperatures in the region effective to plastic collapse. The latter fact might intensify ovalization of elbows in thin-walled pipings used in LMFBR plants.

Acknowledgement

The contributions of Mr. M. Horikiri to the execution of the tests are gratefully acknowledged. The authors wish to express their gratitude for the fruitful comments given by Mr. K. Okabayashi, Dr. T. Kano and Dr. K. Iwata of Power Reactor and Nuclear Fuel Development Corporation (PNC) and Mr. T. Yuhara of Mitsubishi Heavy Industries, Ltd. The concept shown in Fig. 11 was proposed by Mr. R. Miura of Japan Steel Works, Ltd. who worked with authors for creep buckling tests. The work was conducted under the supervision of Mr. M. Hori and Mr. M. Sato of O-arai Engineering Center of PNC.

Reference

- [1] Imazu, A. et al., "Elevated Temperature Elastic-Plastic-Creep Test of an Elbow Subjected to In-Plane Moment Loadings", J. of Pressure Vessel Technology, May 1977.
- [2] Imazu, A. and Nakamura, K., "Simplified Creep Buckling Analysis of Elbows under In-Plane Bending", 5th Int. Conf. on Structural Mechanics in Reactor Technology, F3/5, Aug. 1979.
- [3] Iida, K. et al., "Creep and Relaxation Behaviours of 304 Stainless Steel Piping Elbows", 5th Int. Conf. on Structural Mechanics in Reactor Technology, L13/9, Aug. 1979.
- [4] Greenstreet, W. L., "Experimental Study of Pipe Elbows", ORNL/NUREG-24, Feb. 1978.
- [5] Sobel, L. H. and Newman S. Z., "Instability Analysis of Elbows in the Plastic Range", 4th Int. Conf. on structural Mechanics in Reactor Technology, L3/2, Aug. 1977
- [6] Takeda, H., Asai, S. and Iwata, K., "A New Finite Element for Structural Analysis of Piping Systems", 5th Int. Conf. on Structural Mechanics in Reactor Technology, M5/5, Aug. 1979.
- [7] ASME Boiler and Pressure Vessel Code, 1980.
- [8] Mello, R. M. and Griffin, D. S., "Plastic Collapse Loads for Pipe Elbows Using Inelastic Analysis", J. of Pressure Vessel Technology, Aug. 1974.
- [9] Spence, J. and Findlay, G. E., "Limit Loads for Pipe Bends under In-Plane Bending", 2nd Int. Conf. Pressure Vessel Tech. 1-28.
- [10] Cases of ASME Boiler and Pressure Vessel Code, Case N-47-17.
- [11] Rodabaugh, E. C. and Moore, S. E., "Evaluation of the Plastic Characteristics of Piping Products in Relation to ASME Code Criteria", NUREG/CR-0261, July 1978.

Table 1 Dimensions of Specimens and Test Conditions

Symbol of specimen	Outside dia. (mm) ¹⁾	Radius of bend (mm) ¹⁾	Wall thick. (mm) ¹⁾	Type of loading	Type of test ²⁾	Test temp. (°C)
BE-305	318.5	457.2	6.5	In-plane	PB	600
BE-306	318.5	457.2	6.5	In-plane	PB	600
BE-308A	318.5	457.2	4.5	In-plane	PB	600
BE-308B	318.5	457.2	4.5	In-plane	PB	600
BE-309	318.5	457.2	4.5	Out-of-plane + torsion	PB	600
BE-304	318.5	457.2	6.5	In-plane	CB	600
BE-307	318.5	457.2	6.5	In-plane	CB	600

Note: 1) nominal values 2) PB: plastic buckling, CB: creep buckling

Table 2 Comparison of Collapse Load

Specimen		BE-305	BE-306	BE-308A	BE-308B	BE-309	BE-301
Material		Type 304 stainless steel					Carbon st.
Test temperature		600°C					Room temp.
Outside diameter	Do (mm)	323.6	323.3	320.0	319.8	320.0	318.5
Wall thickness	t (mm)	7.06	7.32	5.16	5.04	4.98	7.10
Radius of bend	R (mm)	457.2	457.2	457.2	457.2	457.2	457.2
Mean radius	r (mm)	158.3	158.0	157.4	157.4	157.5	155.7
Pipe factor	λ	0.1288	0.1341	0.0952	0.0930	0.0918 ²⁾	0.1339
Moment lever ¹⁾	Lm (mm)	1,366	1,366	1,597	1,597	1,061 ²⁾	1,366
C ₂ index	$1.95/\lambda^{3/2}$	7.65	7.44	9.35	9.50	9.58	7.45
B ₂ index	$0.75C_2$	5.74	5.58	7.01	7.13	7.19	5.59
① Plastic instability load	P _I (kgf)	1,650			770	1,200	3,680
② Collapse load	P _C ^A (kgf)	1,170	1,375	570	530	865	3,500
③ Collapse load	P _C ^α (kgf)	1,220	1,405	580	535	870	3,550
④ Collapse load	P _C ^β (kgf)	1,535			765	1,160	3,630
⑤ Collapse load	P _C ^{α2} (kgf)	1,140	1,200	515	450	910	
② ②/①	P _C ^A /P _I	0.71			0.69	0.72	0.95
③ ③/①	P _C ^α /P _I	0.74			0.70	0.73	0.96
④ ④/①	P _C ^β /P _I	0.93			0.99	0.97	0.99
⑤ ⑤/①	P _C ^{α2} /P _I	0.69			0.58	0.76	
⑥ Allow. load for levelD serv.	P _{all} (D)	1,970	2,100	1,000	960	1,420	3,020
⑦ Initial yield load	P _y (kgf)	680	730	350	330	490	1,630
⑧ Limit load for straight pipe	P _{LS} (kgf)	6,670	6,890	4,120	4,030	6,000	15,500
⑨ ②/⑦	P _C ^A /P _y	1.72	1.88	1.63	1.61	1.77	2.15
⑩ ②/⑧	P _C ^A /P _{LS}	0.172	0.200	0.138	0.132	0.144	0.226

Note: 1) distance from loaded end to center of elbow.

2) lever which contributes to out-of-plane moment.

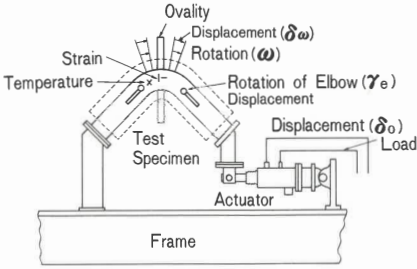


Fig. 1 Set-up for Testing

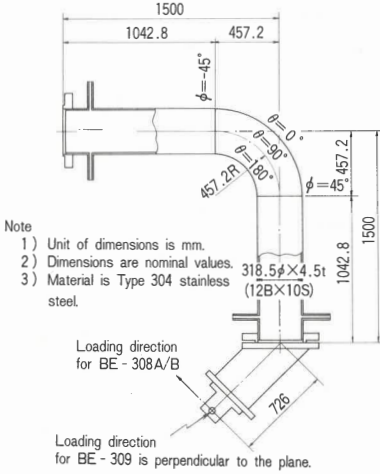


Fig. 2 Specimen Configuration

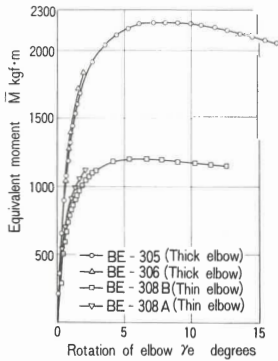


Fig. 3 Relation between Moment and Rotation of Elbow under In-Plane Bending

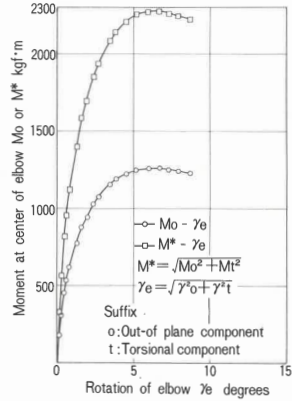


Fig. 4 Relation between Moment and Rotation of Elbow under Out-of-Plane Bending

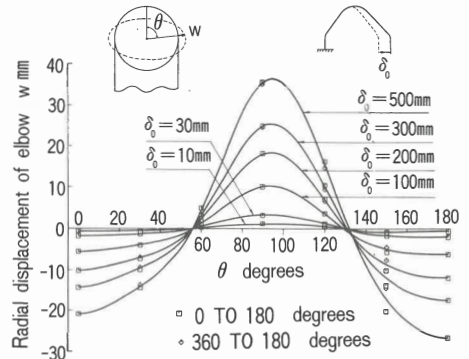


Fig. 5 Distribution of Radial Displacements along Circumference (BE-308B)

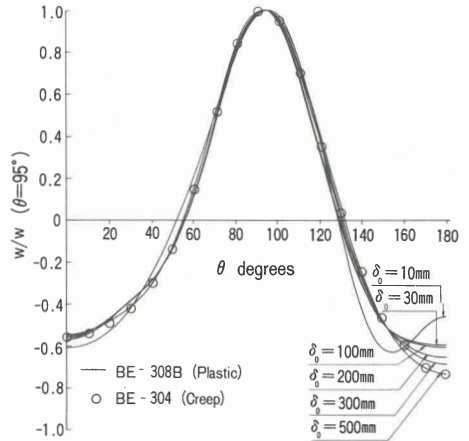


Fig. 6 Distribution of Normalized Radial Displacements

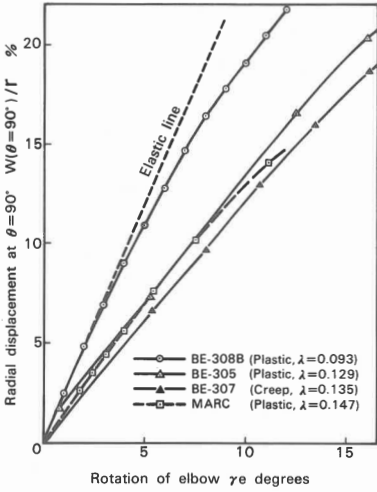


Fig. 7 Relation between Radial Displacement and Rotation of Elbow

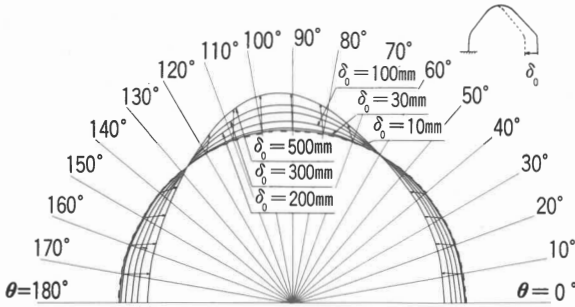


Fig. 9 Change of Cross-Section of Elbow

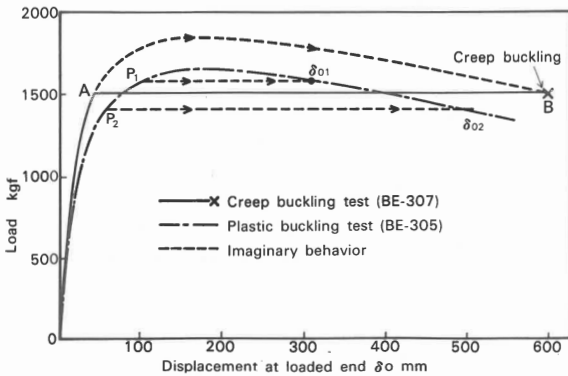


Fig. 11 Comparison of Plastic and Creep Buckling

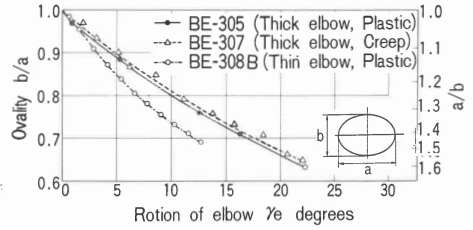


Fig. 8 Relation between Ovality and Rotation of Elbow

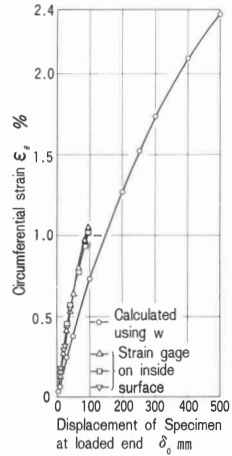


Fig. 10 Change of Strains with End Displacement

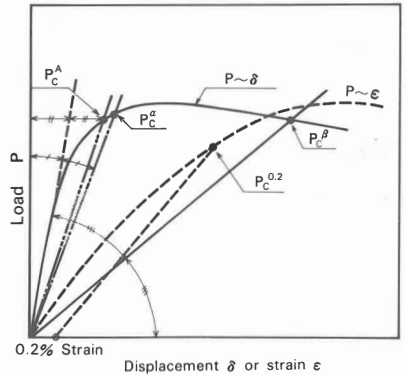


Fig. 12 Definition of Collapse Load